OPTOELECTRONICS AND ADVANCED MATERIALS – RAPID COMMUNICATIONS Vol. 9, No. 9-10, September – October 2015, p. 1264 - 1272

Implementation of FPGA based fuzzy and hysteresis controllers for power quality improvement in single phase three-level rectifier

J. GNANAVADIVEL*, N. SENTHIL KUMAR, S. T. JAYA CHRISTA
Electrical and Electronics Engineering Department, Mepco Schlenk Engineering College, Sivakasi, Tamilndu, India

A diode bridge rectifier with two switches is considered in this paper to convert AC power to three level DC power. The objective of this paper is to design closed loop controllers for AC-DC three level boost converter to achieve unity power factor, reduce source current total harmonic distortion (THD) and regulate output voltage. Hysteresis controller is designed for inner current controller whereas, a PI controller and a fuzzy logic controller are designed for outer voltage controller. The controllers are implemented in Xilinx Spartan-6 XC6SLX25 FPGA board. From hardware and simulation results, proposed fuzzy logic voltage controller with Hysteresis current controller performs well compared to PI voltage controller with Hysteresis current control. The proposed fuzzy logic control is able to achieve high power factor close to unity, source current THD of 3.391% and 91.3% efficiency at rated power.

(Received July 11, 2015; accepted September 9, 2015)

Keywords: FLC, HCC, PI, Power Factor, Total harmonic distortion, Three-level converter

1. Introduction

Diode/thyristor based bridge rectifiers are one of the widely used power supplies. The major drawbacks of the conventional diode bridge rectifier and thyristor based rectifier are low power factor and high current harmonics in ac supply. Inserting an inductor on the ac supply side is a simple method to improve the current waveform but this reduces the power factor [1]-[3]. IEEE 519 and IEC 1000-3-2 standards prescribe the allowable limit of harmonics in the input side [4] [5]. With the increase of power-electronic products, the power factor correction (PFC) becomes important [6]. PFC function includes shaping the current waveform and regulating the output voltage. Due to continuous input current, boost-type converter has been widely integrated to the AC-DC converter to achieve the desired PFC function and harmonic reduction [7].

The conventional multiloop control includes an inner current loop and an outer voltage loop, and it is often used to generate the gate signal for the conventional boost-type AC-DC converter. The inductor current signal is fed back to the inner current loop to shape the current waveform. The output voltage is sensed for the outer loop to regulate the desired output. Sensing input voltage is also required for the generation of the desired current reference [8] [9] and the feed forward terms [10] [11]. In [12] [13], some compensation loops are added to the multiloop control to improve the PFC performance for motor drive applications. For the boost converter, the single switch needs to withstand the overall output voltage when the switch blocks. For high voltage applications, power semiconductor devices with high voltage stress are generally required. To overcome this problem, generally multilevel converters are used for high voltage, high power applications. A conventional single-phase three-level rectifier requires eight power semiconductor switches. The main drawback of this topology is the requirement of more number of semiconductor switches. Hence, in this paper, a single phase AC-DC multilevel converter which requires only two power semiconductor switches is used.

In three-level boost converter, two capacitors are connected across the switches. Thus, each switch needs to withstand only half the output voltage. In addition, the inductor voltage in these boost converter has three levels, but the inductor voltage in the conventional boost converter has only two levels. Therefore, the three-level boost converter is able to yield smaller inductor current ripple than the conventional boost converter. Three-level converters are often used in applications, such as high-voltage–ratio DC/DC conversion [14]-[17] and wide input voltage range [18], especially in the fuel cell applications [16, 18] and grid-connected applications [15] [19] [20].

Additionally, the high withstanding voltage semiconductor switches often have larger Drain-Source resistances than the low withstanding voltage ones. Thus, the three-level converter has the advantages of the low voltage stress, the small inductor current ripple and the low switching loss [6][16][21]. The three-level AC-DC converter was obtained by connecting the diode rectifier with the three-level DC-DC converter [22]-[25],[29][30]. Recently, Fuzzy logic controller is used to generate the control signals for power converters. In [26]-[27], FLC is used in DC-DC converter and also used in two level AC-DC converter [28]. PI with Hysteresis current control technique adopted in [24], claimed to have achieved 6%

Total Harmonic Distortion in source current and the power factor closer to unity. The IEEE-519 standard specifies that the current THD should be less than 5%.

In this paper, fuzzy logic voltage control is proposed for the single-phase three-level AC-DC converter. However, two control strategies such as PI voltage controller with hysteresis current controller and fuzzy logic voltage controller with hysteresis current controller are implemented for the converter with the objectives of drawing a pure sinusoidal input current with low total harmonic distortion and high power factor. The performances of the proposed fuzzy control scheme are also compared with PI control scheme. The proposed AC-DC converter can be used as a front stage for battery charger, uninterrupted power supply, and three-level inverter applications. This manuscript suggested improved fuzzy logic voltage controller with hysteresis control method by which compared to [24], lesser source current Total Harmonic Distortion of 3.391% can be achieved and also power factor closer to unity. Also the Total Harmonic Distortion achieved is lesser than the IEEE-519 standard limit.

2. AC-DC three level converter and its modeling

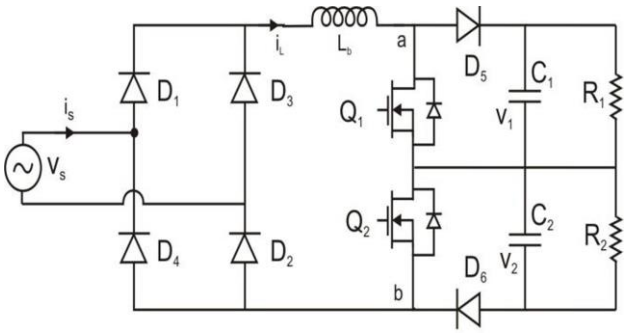

Fig. 1. Circuit configuration of single-phase ac-dc multilevel converter.

Fig. 1 shows the single phase ac-dc three level converter. This circuit strategy consists of a single phase diode bridge rectifier, two power switching devices, one inductor, two fast recovery diodes and two dc capacitors. An inductor L_b is used to reduce current ripple. The voltage rating of the power semiconductors are reduced to half of dc bus voltage. The inductor boost volume is one quarter of the conventional boost converter. The single phase three level rectifier can be analyzed in its four operating modes according to the states of two power semiconductor switches Q_1 and Q_2 [22-25].

From the circuit diagram, when Q_1 and Q_2 are ON, the modeling equations are

$$v_s = L_b \frac{di_L}{dt} \tag{1a}$$

$$C_1 \frac{dv_1}{dt} = -\frac{v_1}{R_1} \tag{1b}$$

$$C_2 \frac{dv_2}{dt} = -\frac{v_2}{R_2} \tag{1c}$$

From the circuit diagram, when Q_1 is ON and Q_2 is OFF, the modeling equations are

$$L_b \frac{di_L}{dt} = v_s - v_2 \tag{2a}$$

$$C_1 \frac{dv_1}{dt} = -\frac{v_1}{R_1} \tag{2b}$$

$$C_2 \frac{dv_2}{dt} = i_L - \frac{v_2}{R_2} \tag{2c}$$

From the circuit diagram, when Q_1 is OFF and Q_2 is ON, the modeling equations are

$$L_b \frac{di_L}{dt} = v_s - v_1 \tag{3a}$$

$$C_1 \frac{dv_1}{dt} = i_L - \frac{v_1}{R_1} \tag{3b}$$

$$C_2 \frac{dv_2}{dt} = i_L - \frac{v_2}{R_2} \tag{3c}$$

From the circuit diagram, when Q_1 and Q_2 are OFF, the modeling equations are

$$L_b \frac{di_L}{dt} = v_s - v_1 - v_2 \tag{4a}$$

$$C_1 \frac{dv_1}{dt} = i_L - \frac{v_1}{R_1} \tag{4b}$$

$$C_2 \frac{dv_2}{dt} = i_L - \frac{v_2}{R_2} \tag{4c}$$

Averaging equations 1,2,3 and 4, over one switching period, we get

$$L_b \frac{di_L}{dt} = v_s - v_0\left(1 - d_1 - \frac{d_2}{2}\right) \tag{5a}$$

$$C_1 \frac{dv_1}{dt} = i_L\left(1 - d_1 - \frac{d_2}{2}\right) - \frac{v_1}{R_1} \tag{5b}$$

$$C_2 \frac{dv_2}{dt} = i_L\left(1 - d_1 - \frac{d_2}{2}\right) - \frac{v_2}{R_2} \tag{5c}$$

Perturb the averaged equations 5 assuming,

$$v_s = V_s + \hat{v}_s \qquad v_1 = V_1 + \hat{v}_1 \qquad v_2 = V_2 + \hat{v}_2$$

$$i_L = I_L + \hat{i}_L \qquad d = D + \hat{d} \qquad d = d_1 = 0.5d_2$$

Where, d_1=duty cycle of switch Q_1 and d_2=duty cycle of switch Q_2

Upon simplification we could arrive transfer function of three level boost converter as,

$$\frac{\hat{v}_0(s)}{\hat{d}(s)} = \frac{v_0(1-D) - sL_bI_L}{s^2L_bC + \frac{sL_b}{R} + (1-D)^2} \quad (6)$$

Table 1. Design specifications and circuit parameters

S.No	Parameter	Specification
1	Input line voltage (V_s)	28 V
2	Output voltage	48 V
3	Output power	100 W(50×2)
4	Switching frequency (f_s)	10 kHz
5	Duty cycle (D)	0.33
6	Line frequency	50 Hz
7	Boost inductor (L_b)	3 mH
8	Capacitance C_1=C_2	2000 µF
9	Load resistance	23 Ω(11.5×2)

Table 1 gives the design specification of the 100W prototype converter built for testing.

By substituting the values from Table 1 in the equation (6), we get

$$\frac{\hat{v}_o(s)}{\hat{d}(s)} = \frac{32.16 - 11.1\times10^{-3}s}{10.5\times10^{-7}s^2 + 0.13\times10^{-3}s + 0.4489} \quad (7)$$

This transfer function is used for the design of controller.

3. Design of controllers

The proposed block diagram of the single-phase AC-DC three level converter is shown in Fig. 2. This system consists of three level ac-dc converter, voltage controller, power estimator, compensated capacitor selector, region selector, current controller and switching table. The proposed closed loop control has two loops. One is outer voltage control loop and other one is inner current loop. In outer voltage control loop, the converter output voltage is sensed and compared with the reference voltage. After comparison, error signal is fed to the PI controller. The supply voltage is rectified in order to produce absolute value of sinωt. The power estimator output, PI controller output and absolute value of sin ωt are used to obtain the amplitude of reference inductor current. This reference inductor current is compared with actual inductor current. After comparison, error signal is fed to the inner current control loop. This controller generates one control signal (b_3). In this current controller, hysteresis control is implemented. Region selector is used to find whether the rectified output voltage is in region 1 or 2 and also helps to provide one control signal (b_1) to generate the switching signals [23]. Compensated capacitor selector is used to find the capacitor to be compensated under unbalance condition among two bus capacitors and also helps to provide one of the control signals (b_2) to generate the switching signals. The two power semiconductor switching devices are controlled based on a switching table – Table 3.

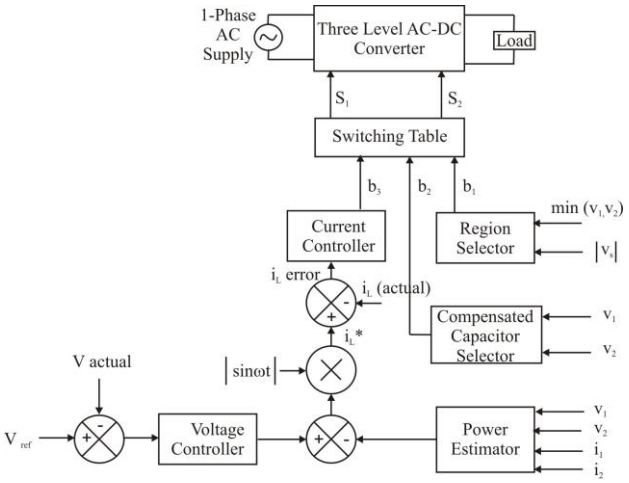

Fig. 2. Proposed block diagram of single-phase ac-dc multilevel converter.

3.1 Design of PI voltage controller

The PI controller takes into account the desired output of the converter to produce control signal which is necessary to reduce the error signal approximately to zero. A proportional controller gain (K_p) has the effect of reducing the rise time and does not eliminate the steady state error. An integral control gain (K_i) has the effect of eliminating the steady state error but makes the transient response worse. From the transfer function of three-level boost converter, proportional gain and integral gain values are obtained by using MATLAB auto tuning. The values are K_p=0.163 and K_i=0.9. This PI controller is used in the voltage loop for regulating the desired voltage.

Region selector is used to find whether the rectified output voltage is in region 1 or 2 and also helps to provide one control signal (b_1) to generate the switching signals. Region selector is based on the following condition.

$$b_1 = \begin{cases} 1, & |v_s| > \min(v_1, v_2) \\ 0, & |v_s| < \min(v_1, v_2) \end{cases} \quad (8)$$

Compensated capacitor selector is used to find which capacitor is to be compensated under unbalance condition among two bus capacitors and also helps to provide one of the control signals (b_2) to generate the switching signals. Compensated capacitor selection is based on the following condition.

$$b_2 = \begin{cases} 1, & v_1 > v_2 \\ 0, & v_1 < v_2 \end{cases} \quad (9)$$

The supply voltage is rectified in order to produce absolute value of sinωt. The dc-link voltage regulator,

power estimator output and absolute value of sinωt are used to obtain the amplitude of reference inductor current. The reference inductor current is given by

$$i_L^* = \left(\frac{2(v_1 i_1 + v_2 i_2)}{v_{s.peak}} + K_p v_{err} + K_i \sum v_{err} \right) |\sin \omega t| \quad (10)$$

where, K_P–Proportional gain, K_i-Integral gain

$$v_{err} = v_{dc}^* - v_{dc} \quad (11)$$

where, v^*_{dc} – Reference output voltage, v_{dc} – Actual output voltage.

3.2 Design of Hysteresis current controller

The inductor current variation is a function of the rectified supply voltage $|V_s|$ and the dc side voltage $V_{ab.}$ If the desired inductor current, capacitor voltage, rectified supply voltage are known, a proper operation mode can be selected to control the inductor current to follow the current command and to compensate capacitor voltages. In this paper, two controllers are used. One is Hysteresis current controller [23][24] and another one is proposed Fuzzy logic current controller. The inductor current error is expressed as,

$$\Delta i_L = i_L^* - i_L \quad (12)$$

where i_L* is the reference inductor current which is in phase with the rectified supply voltage, i_L is actual inductor current. If the error in the inductor current is controlled within the preset band h, the inductor current will follow reference current with a limited current distortion and the current error is fed into the hysteresis comparator to select a proper operating mode for compensating the actual inductor current and for charging or discharging the capacitor voltage. To maintain a good voltage waveform, the voltage balance problem of capacitor is considered in the proposed control scheme.

$$b_3 = \begin{cases} 1, & i_L^* - i_L > h \\ 0, & i_L^* - i_L < -h \end{cases} \quad (13)$$

In this controller, the hysteresis band value is 0.15.

3.3 Design of Fuzzy logic voltage controller

The fuzzy logic controller is proposed to handle the nonlinear properties of single phase ac-dc three level converter under variable operating conditions. The fuzzy logic controller is used as a voltage controller. Power estimator, fuzzy logic controller output and absolute value of sinωt are used to generate the reference inductor current. Reference inductor current is compared with the actual inductor current. The calculated error in inductor current is given as the input to the hysteresis controller. PI like fuzzy logic controller is used as voltage regulator which takes two inputs such as output voltage error and integral of voltage error and output is reduction of error. Mamdani type fuzzy inference system is enabled.

Table 2 shows the fuzzy control rules. Two input variables (error and change in error) and one output variable (controlled voltage signal) are used in the design the fuzzy logic controller. Fig.3 Shows the Membership functions for the input 1 (error), input 2 (change in error) and output (control voltage signal). The membership functions for the input and output variables are designed such that converter performance is improved. Centroid method is used for defuzzification.

Table 2. Fuzzy control rules

CE / E	NB	NM	NS	Z	PS	PM	PB
NS	Z	PS	PM	PB	PB	PB	PB
PM	NS	Z	PS	PM	PB	PB	PB
PS	NM	NS	Z	PS	PM	PB	PB
Z	NB	NM	NS	Z	PS	PM	PB
NS	NB	NB	NM	NS	Z	PS	PM
NM	NB	NB	NB	NM	NS	Z	PS
NB	NB	NB	NB	NB	NM	NS	Z

NB- Negative Big, NM-Negative Medium, NS-Negative Small, Z-Zero, PS-Positive Small, PM-Positive Medium, PB-Positive Big.

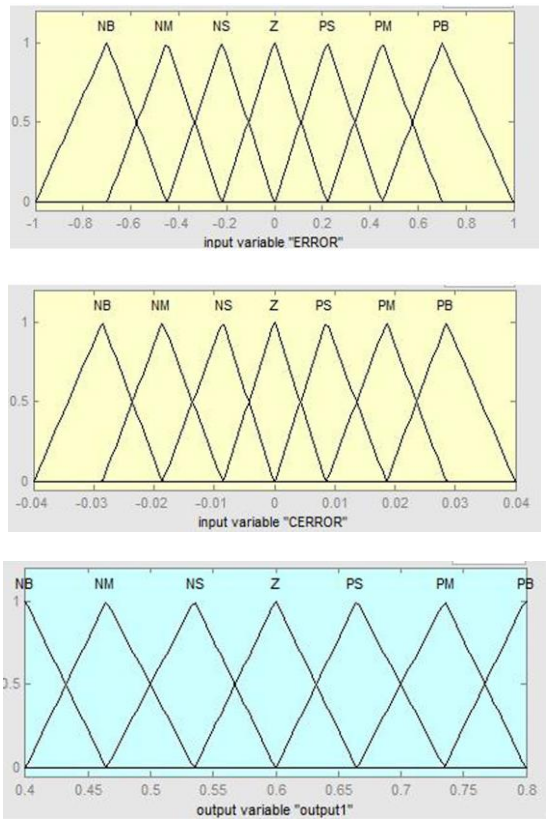

Fig. 3. The Membership functions for the input 1 (error), input 2 (change in error) and output (control current signal).

4. Simulation of the systems

The proposed power circuit, PI voltage controller, Hysteresis current controller and Fuzzy logic voltage controller are simulated in MATLAB/SIMULINK.

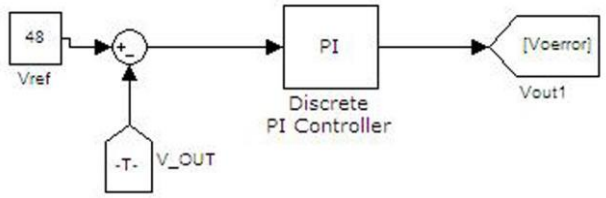

Fig. 4a. Simulink model of PI voltage controller.

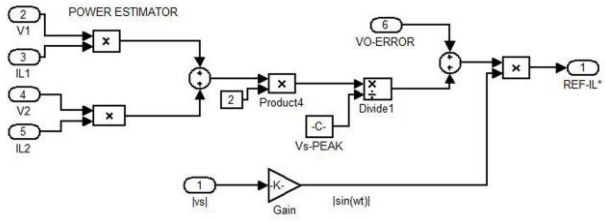

Fig. 4b. Simulink model of reference inductor current generation.

Fig. 4a shows the simulink model of PI voltage controller.the reference voltage is compared with actual voltageby using comparator. The output of the comparator is fed to the PI controller block. The PI controller produces the error signal V_{oerror} . Fig.4b. shows the simulink model of reference inductor current generation. The reference inductor current is generated by using power estimator, output from the PI controller and absolute value of sinωt. The reference inductor current is generated and compared with actual inductor current to get inductor current error.

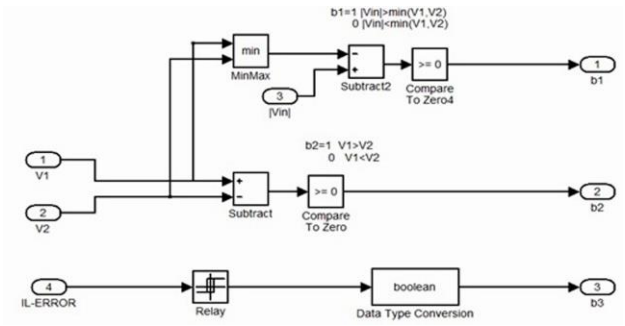

Fig. 4c. Simulink model for control signal generation with HCC.

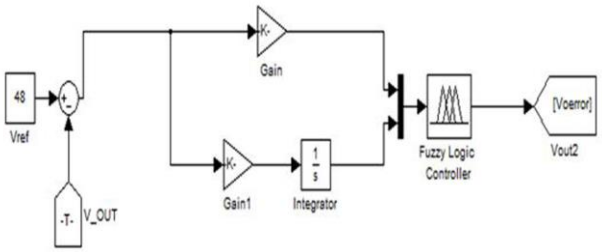

Fig. 4d. Simulink model for control Fuzzy Logic voltage controller.

Fig. 4c. shows simulink model for control signal generation with HCC. Fig. 4d shows the simulink model fuzzy logic voltage control. The switching states of two switches Q_1 and Q_2 are varied according to the switching table (Table 3). NAND gates are used to implement this switching table as shown in Fig.5.

Table 3. Relations between the switching signals (Q_1, Q_2) and control signals (b_1, b_2, b_3)

b_1	b_2	b_3	Q_1	Q_2
0	0	0	0	1
0	0	1	1	1
0	1	0	1	0
0	1	1	1	1
1	0	0	0	0
1	0	1	0	1
1	1	0	0	0
1	1	1	1	0

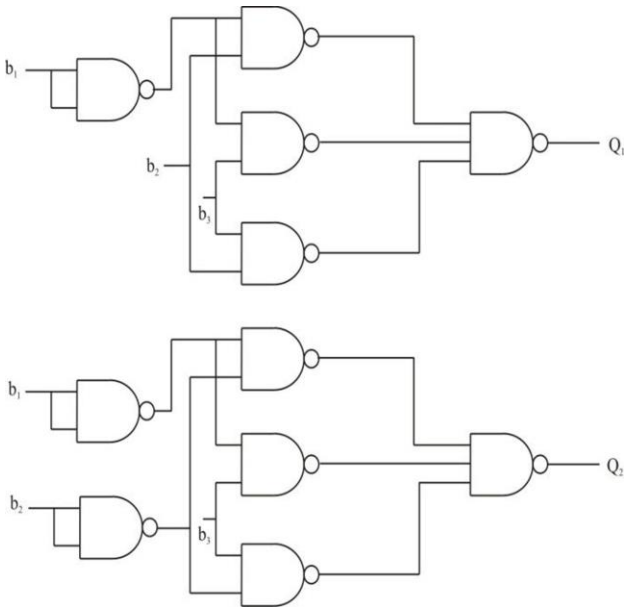

Fig. 5. Implementation of switching table (TABLE 3) using NAND gates.

5. Simulation results of proposed system

The PI outer loop voltage controller with Hysteresis inner loop current controller and proposed Fuzzy logic outer loop voltage controller with Hysteresis inner loop current controller techniques are simulated through MATLAB Simulink.

5.1 Simulation results with PI voltage controller and Hysteresis current controller

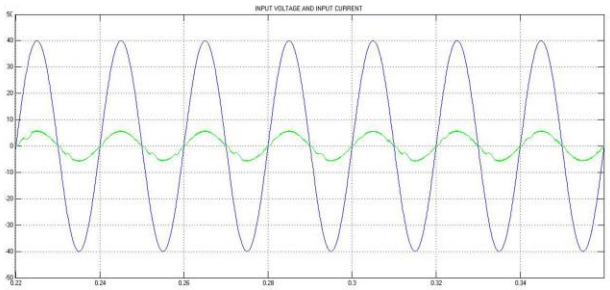

Fig. 6a. Input voltage and input current waveforms with PI voltage controller and Hysteresis current controller.

Fig. 6a. shows the input voltage and input current waveforms for system with PI and HCC. Here, input voltage and input current waveforms are in phase. Therefore the input power factor of the circuit is almost unity. But the input current waveform is slightly distorted. The total Harmonic Distortion of input current waveform is 7.27%. Fig. 6b shows the FFT analysis of the input current waveform.

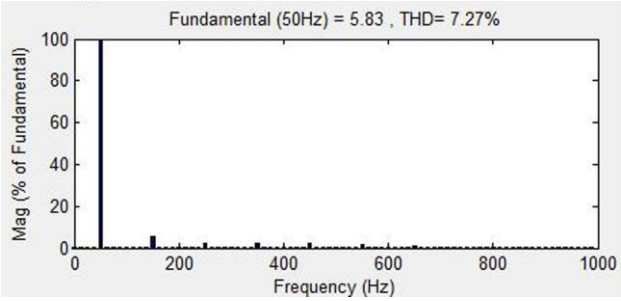

Fig. 6b. Harmonic spectrum of input current waveform with PI and HCC.

Table 4. Performance analysis under variation of load power with Hysteresis current controller

Output Power (Watts)	Output Voltage (V)	Source Current THD (%)	Power Factor	Efficieny (%)
70	48	13.56	0.9816	79.8
80	48	11.29	0.9883	81
90	48	8.6	0.9905	85.2
100	48	7.27	0.9948	88.66

Table 4 shows that, if the output power of the load is varied (increased from 70 W to 100 W) the output voltage is almost constant. THD is decreased from 13.56% to 7.27% and power factor is increased from 0.986 to 0.9970. The efficiency of the converter is increased from 79.8% to 88.66% as the load power is increased.

5.2 Simulation results with proposed Fuzzy logic voltage controller and Hysteresis current controller

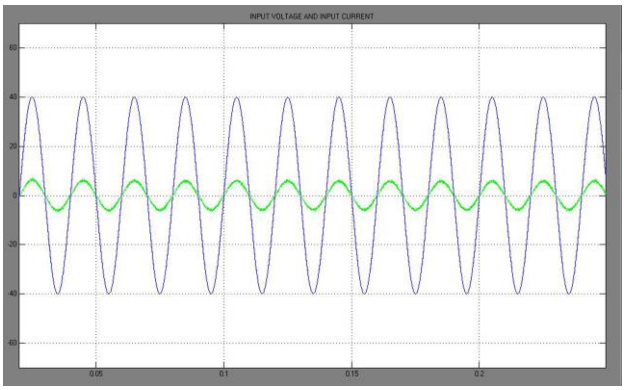

Fig. 7a. Input voltage and input current waveforms with Fuzzy logic voltage controller and Hysteresis current controller.

Fig. 7a. shows the input voltage and input current waveforms for PI voltage controller and with FL current controller. Here, input voltage and input current waveforms are almost in phase. Therefore the input power factor of the circuit is near unity. The total Harmonic Distortion of input current waveform is 3.11% at rated power of the converter. Fig. 7b shows the FFT analysis of the input current waveform.

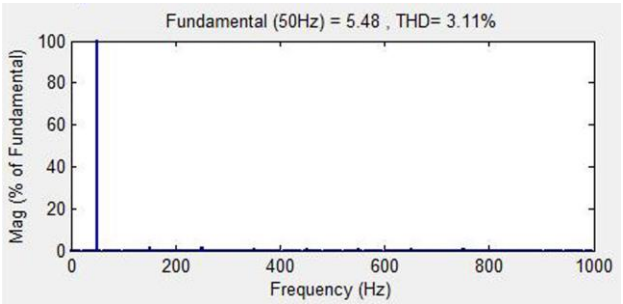

Fig. 7b. Harmonic spectrum of input current waveform with Fuzzy logic voltage controller and Hysteresis current controller.

Table 5. Performance analysis under variation of load power

Output Power (Watts)	Output Voltage (V)	Source Current THD (%)	Power Factor	Efficieny (%)
70	48	4.2	0.9991	87.9
80	48	3.9	0.9993	90.2
90	48	3.3	0.9994	91.1
100	48	3.11	0.9998	92.5

Table 5 shows, if the output power of the load is varied (increased from 70 W to 100 W) the output voltage almost constant. THD is decreased from 4.2% to 3.11%. Power factor of the circuit is almost unity. The efficiency of the converter will increased from 89% to 92.5%. The THD at rated power is reduced to less than 5% which is the prescribed IEEE-516 standard.

6. FPGA implementation

Fig. 8 shows the proposed hardware setup proposed system. The design of controllers is implemented using VHDL language in Xilinx Spartan-6 XC6SLX25 FPGA board. From the circuit, the various parameters such as capacitor voltages v_1 and v_2, load currents i_{L1} and i_{L2}, actual inductor current and source voltage are sensed and given to ADC as an input. The converted digital signals are given to the FPGA based control board. The PI control is used as a voltage controller. The FLC is used as a current controller. Based on the control algorithm, FPGA generates two gating signals. These gating signals are fed to the single phase three level rectifier through gate drive circuit.

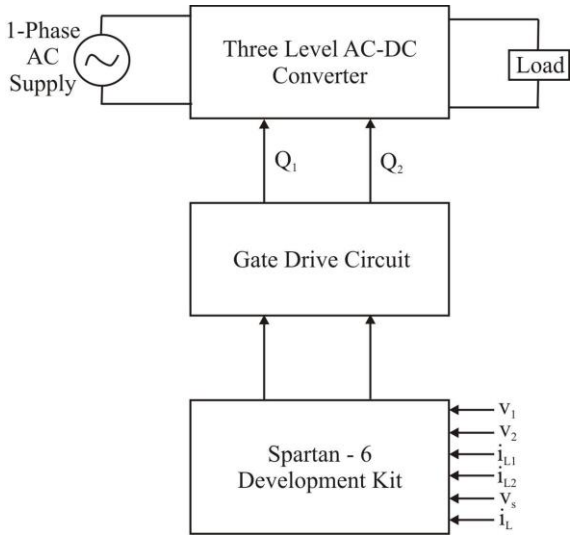

Fig. 8. Proposed hardware block diagram.

6.1 Experimental results

To verify the validity of the proposed fuzzy logic voltage controller and hysteresis current controller compared with PI voltage controller and hysteresis current controller for single phase three level ac-dc converter has been built and tested in the laboratory as shown in Fig.9a.

Fig. 9a. Hardware setup

The power devices and various components of the prototype are Input rectifier bridge-MUR360, Power switches - IRF250, Boost inductor - 3mH, Output filter capacitor -2200µF, Controller - FPGA Spartan-6, Voltage sensor -HCPL-7840, Hall effect current sensor - WCS 2705 and Load resistor – (11.5Ω×2).

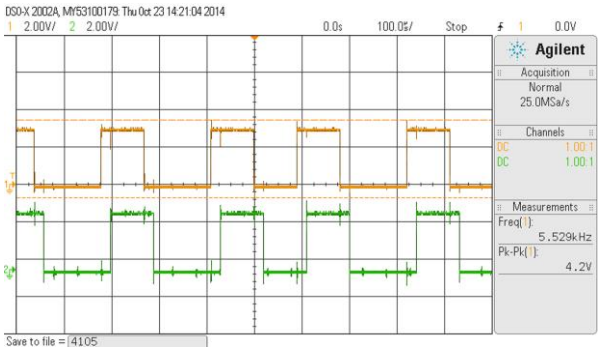

Fig. 9b. Gate pulse waveform generated from FPGA.

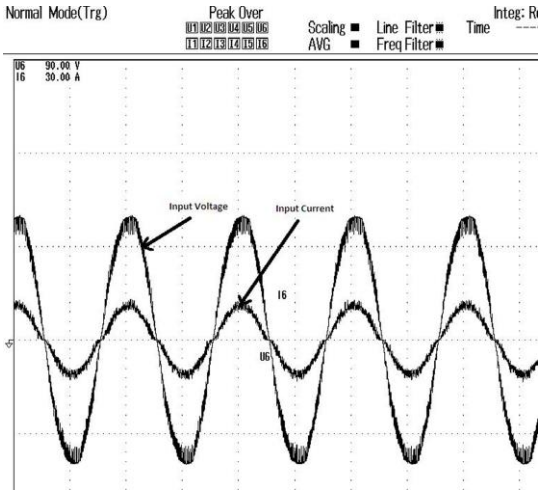

Fig. 10a. Experimental input voltage and input current waveforms at rated power with PI voltage controller and Hysteresis current controller.

Normal Mode | Peak Over | Scaling | Line Filter | Freq Filter | Time | Integ: Reset

	Element 1	Element 2	Element 3	Element 4	Element 5	Element 6
Urms [V]	0.00	0.00	0.00	0.00	0.00	28.115
Irms [A]	0.0000	0.0000	0.0000	0.000	0.000	3.937
P [W]	-0.00	-0.00	-0.00	-0.0000k	-0.0000k	109.35
S [VA]	0.00	0.00	0.00	0.0000k	0.0000k	111.52
Q [var]	0.00	0.00	0.00	0.0000k	0.0000k	21.92
λ [ ]	Error	Error	Error	Error	Error	0.9805
S [VA]	0.00	0.00	0.00	0.0000k	0.0000k	111.52
Uthd [%]	90.541	98.403	99.445	98.857	98.132	4.171
Ithd [%]	80.053	99.983	99.868	99.880	99.393	7.562

Fig. 10b. Power Quality measurements in element 6 for rated load power with PI voltage controller and Hysteresis current controller.

Fig. 9b shows the experimental waveforms of the gating pulses of power switches Q_1 and Q_2. These pulses are obtained from FPGA. Fig. 10a. shows the experimental waveforms of input voltage and input current for rated load power with PI voltage and hysteresis current controller. Power factor and THD are measured from power quality analyzer shown in Fig. 10b. From this Fig.10b. the input power factor is 0.9805 and THD is 7.562%.

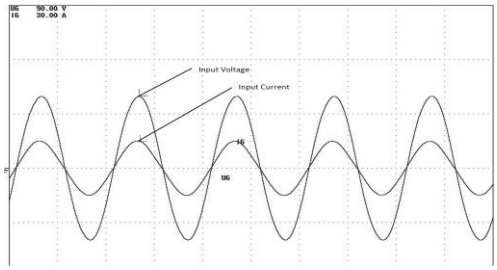

Fig. 11a. Experimental input voltage and input current waveforms at rated power with Fuzzy logic voltage controller and Hysteresis current controller.

Normal Mode | Peak Over | Scaling | Line Filter | Freq Filter | Time | Integ: Reset

8 change items

	Element 1	Element 2	Element 3	Element 4	Element 5	Element 6
Urms [V]	0.00	0.00	0.00	0.00	0.00	28.159
Irms [A]	0.0000	0.0000	0.0000	0.000	0.000	3.8974
P [W]	-0.0000k	-0.0000k	-0.0000k	0.0000k	-0.0000k	109.56
S [VA]	0.0000k	0.0000k	0.0000k	0.0000k	0.0000k	110.09
Q [var]	0.0000k	0.0000k	0.0000k	0.0000k	0.0000k	10.77
λ [ ]	Error	Error	Error	Error	Error	0.9952
S [VA]	0.0000k	0.0000k	0.0000k	0.0000k	0.0000k	110.09
Uthd [%]	75.660	91.600	93.530	98.724	99.986	1.807
Ithd [%]	96.069	99.284	99.470	99.932	98.859	3.391

Fig. 11b. Power Quality measurements in element 6 for rated load power with Fuzzy logic voltage controller and Hysteresis current controller.

Fig. 11a. shows the experimental waveforms of input voltage and input current for rated load power with Fuzzy logic voltage controller and Hysteresis current controller. Power factor and THD are measured from power quality analyzer shown in Fig.11b. From this Fig.11b, the input power factor is 0.9949 and THD is 3.391.

7. Results and discussion

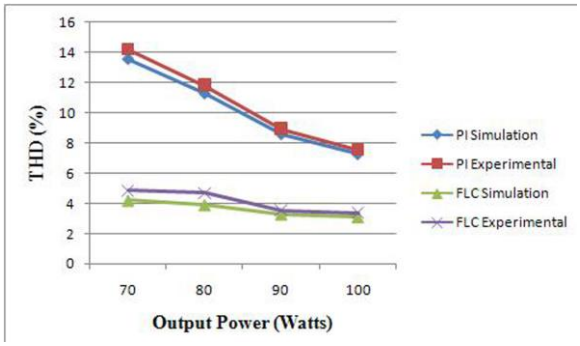

Fig. 12a. Experimental result with comparison of THD value.

Fig. 12a shows total harmonic distortion comparison curve for PI and FLC. From the Fig.12a., the proposed Fuzzy logic controller based single phase AC-DC three level converter gives better results compared with PI voltage controller. THD of the Fuzzy logic voltage controller and Hysteresis current controller is 3.11%. The THD experimental result of FLC with HCC is 3.391%. This value is less than the IEEE-516 standard.

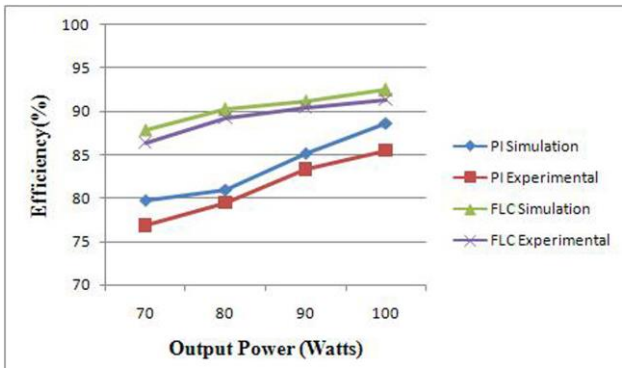

Fig. 12b. Experimental result with comparison of efficiency.

Fig. 12b shows efficiency comparison curve for PI and FLC. From the Fig.12b, it is concluded that Fuzzy logic controller based single phase AC-DC three level converter gives better results compared to PI and HCC. Efficiency of the Fuzzy logic voltage controller and Hysteresis current controller is 92.5%. The efficiency experimental result of FLC with HCC is 91.44%. Fig. 12c shows power factor comparison curve for HCC and FLC. From the Fig. 12c, it is concluded that Fuzzy logic

controller based single phase AC-DC three level converter gives better results compared to PI and Hysteresis current controller. Power factor of the Fuzzy logic voltage controller and Hysteresis current controller is 0.9999. The power factor of experimental result with Fuzzy logic voltage controller and Hysteresis current controller is 0.9949.

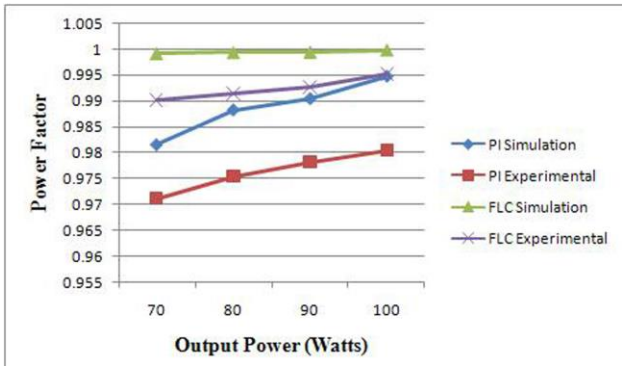

Fig. 12c. Experimental result with comparison of power factor.

8. Conclusion

The paper deals with the design and implementation of closed loop controllers for single phase AC-DC three level converter. The closed loop control for the converters consists of two loops-one outer voltage controller and the other inner current controller. HCC controller is used as a inner current controller. For outer voltage controllers, two controllers are designed-one PI controller and the other fuzzy logic controller. The performance of the entire system is simulated and compared for the two different voltage controllers. The same has been implemented in a FPGA based hardware platform. The comparison reveals that Fuzzy logic voltage controller with Hysteresis current controller has better performance and is able to achieve input current THD of less than 5%. This source current THD is less than that of IEEE-516 standard. An increase in power factor and efficiency is also reported for the proposed fuzzy logic controller.

References

[1] M. M. Jovanovic, D. E. Crow, IEEE Trans. Ind. Applicat., **33**, 551 (1997).
[2] R. Redl, Proc. IEEE Appl. Power Electron. Conf. (APEC), 454 (1998).
[3] A. R. Prasad, P. D. Ziogas, S. Manias, IEEE Trans. Ind. Electron., **37**, 521 (1990).
[4] Limits for Harmonic Current Emissions (Equipment Input Current <16A per Phase), IEC 1000/3/2 Int. Std., (1995).
[5] IEEE 519 Recommended practices and requirements for harmonic control in electrical power systems, Tech. Rep., IEEE Industry Applications Soc./Power Engineering Soc., (1993).
[6] B. Singh, B. N. Singh, A. Chandra, K. Al-Haddad, A. Pandey, D. P. Kothari, IEEE Trans. on Industrial Electronics, **50,** 962 (2003).
[7] J. C. Crebier, B. Revol, J. P. Ferrieux, IEEE Trans. on Industrial Electronics, **52**, 36 (2005).
[8] S. Moon, L. Corradini, D. Maksimovic, IEEE Trans. On Power Electronics, **26**, 3006 (2011).
[9] A. El Aroudi, M. Orabi, R. Haroun, L. Martinez-Salamero, **58**, 3448 (2011).
[10] M. Chen, J. Sun, IEEE Trans. on Power Electronics, **21**, 338 (2006).
[11] H. C. Chen, H. Y. Li, R. S. Yang, IEEE Trans. on Power Electronics, **24**, 1428 (2009).
[12] H. C. Chang, C. M. Liaw, IEEE Trans.on Industrial Electronics, **58**, 1763 (2011).
[13] J. Y. Chai, Y. H. Ho, Y. C. Chang, C. M. Liaw, IEEE Trans. on Industrial Electronics, **55**, 2576 (2008).
[14] L. S. Yang, T. J. Liang, H. C. Lee, J. F. Chen, IEEE Trans. on Industrial Electronics, **58**, 4196 (2011).
[15] Kasinathan Pounraj, Rajasekaran Vairamani, and Selvaperumal Sundramoorthy, IET Power Electronics, **5**, 843 (2013).
[16] A. Shahin, M. Hinaje, J. P. Martin, S. Pierfederici, S. Rael, B. Davat, IEEE Trans. on Industrial Electronics, **57**, 3944 (2010).
[17] E. Ribeiro, A. J. M. Cardoso, C. Boccaletti, IEEE Trans. on Power Electronics, **28**, 3008 (2013).
[18] M. H. Todorovic, L. Palma, P. N. Enjeti, IEEE Trans. on Industrial Electronics, **55**, 1247 (2008).
[19] J. M. Kwon, B. H. Kwon, K. H. Nam, IEEE Trans. on Power Electronics, **23**, 2319 (2008).
[20] V. Yaramasu, B. Wu, Energy Conversion Congress and Exposition (ECCE), 561 (2011).
[21] M. T. Zhang, Y. Jiang, F. C. Lee, M. M. Jovanovic, IEEE APEC **95**, 434 (1995).
[22] R. Greul, S. D. Round, J. W. Kolar, IEEE Trans. on Power Electronics, **21**, 1637 (2006).
[23] B. R. Lin, H. H. Lu, IEEE Trans. on Aerospace and Electronic Systems, **36**, 189-200 (2000).
[24] B. R. Lin, H. H. Lu, IEEE Trans. on Industrial Electronics, **47**, 245 (2000).
[25] H. Wu, X. He, IEEE Trans. Power Electronics, **17**, 946 (2002).
[26] N. Senthil Kumar, V. Sadasivam, H. M. Asan Sukriya, Electric Power Components and Systems, **36**, 680 (2008).
[27] Prema Kannan, Senthil Kumar Natarajan, and Subhransu Sekhar Dash, Mathematics problems in Engineering, Hindawi Publishing Corporation, Article ID 590861, 10 pages (2013).
[28] A. Kessal, L. Rahmani, M. Mostefai, J. Gaubert, Electronics and Electrical Engineering – Kaunes: Technologija, **2**, 67 (2012).
[29] M. Rajesh, B. Singh, IET power Electronics, **7**, 1499 (2014).
[30] Hung-Chi Chen, Jhen-Yu Liao, IEEE Transactions on Industrial Electronics, **61**, (2014).

*Corresponding author: jgvadivel@gmail.com, gnanavadivelj@gmail.com